The Multiscale Discontinuous Galerkin Method for Solving a Class of Second Order Elliptic Problems with Rough Coefficients

Wei Wang*, Johnny Guzmán†and Chi-Wang Shu‡

October 29, 2009

Abstract

We develop a multiscale discontinuous Galerkin (DG) method for solving a class of second order elliptic problems with rough coefficients. The main ingredient of this method is to use a non-polynomial multiscale approximation space in the DG method to capture the multiscale solutions using coarse meshes without resolving the fine scale structure of the solution. Theoretical proofs and numerical examples are presented in both one and two dimensions. For one-dimensional problems, optimal error estimates and numerical examples are shown for arbitrary order approximations. For two-dimensional problems, numerical results are presented by high order multiscale DG method, but the error estimate is proven only for the second order method.

Key words: multiscale discontinuous Galerkin method, rough coefficients

1 Introduction

In this paper, we consider solving a class of second order elliptic boundary value problems with highly oscillatory coefficients. Such equations arise in, e.g. composite materials and porous media. The solution oscillates rapidly and requires a very refined mesh to resolve. It is numerically difficult for traditional numerical methods to do it due to the tremendous amount of computer memory and CPU time. Recently developed multiscale finite element methods [3, 12, 2, 13, 14, 11, 6, 18] provide an idea of constructing multiscale bases which are adapted to the local properties of the differential operators, allowing adequate resolution on a coarser mesh.

In particular, we are interested in the second order elliptic boundary value problems

$$-\nabla \cdot (A(\mathbf{x})\nabla u) = f(\mathbf{x}) \quad \text{in } \Omega \tag{1}$$

*Center for Turbulence Research, Stanford University, Stanford, CA 94305. E-mail: weiwang1@stanford.edu.

†Division of Applied Mathematics, Brown University, Providence, RI 02912. E-mail: jguzman@dam.brown.edu. Research partially supported by NSF grant DMS-0914596.

‡Division of Applied Mathematics, Brown University, Providence, RI 02912. E-mail: shu@dam.brown.edu. Research partially supported by DOE grant DE-FG02-08ER25863 and NSF grant DMS-0809086.

with the boundary condition

$$u = 0 \quad \text{on } \partial\Omega,$$

where Ω is a rectangular domain, f is a function in $L^2(\Omega)$ and $A(\mathbf{x})$ is the coefficient matrix containing small scales.

In applications, Eq. (1) is the pressure equation in modeling two phase flow in porous media (see [15, 13, 6]), with u and $A(\mathbf{x})$ interpreted as the pressure and the relative permeability tensor. Especially when the stochastic permeabilities are upscaled, $A(\mathbf{x})$ is a diagonal tensor. Eq. (1) is also the equation of steady state heat (electrical) conduction through a composite material, with $A(\mathbf{x})$ and u interpreted as the thermal (electric) conductivity and temperature (electric potential) (see [13]).

In the one dimensional case, $A(\mathbf{x}) = a(x)$ and the equation becomes

$$-(a(x)u_x)_x = f(x). \tag{2}$$

In the two dimensional case, we consider A with the following special form

$$A(\mathbf{x}) = \begin{pmatrix} a(x) & 0 \\ 0 & b(y) \end{pmatrix},$$

and the two dimensional equation is

$$-(a(x)u_x)_x - (b(y)u_y)_y = f(x, y). \tag{3}$$

Notice that we are considering this special class of two dimensional problems for the convenience of explicitly constructing multiscale bases, thereby making the multiscale algorithm efficient. The typical situation in multiscale modeling, has $a(x) = a^\varepsilon(x, \varepsilon)$ and $b(y) = b^\varepsilon(y, \varepsilon)$ being oscillatory functions involving a small scale ε. Unlike the work for continuous finite elements in [13, 14, 11, 6], we do not need the assumption of the periodicity of a^ε and b^ε in the ε scale and we do not assume any scale separation. We only assume $a(x)$ and $b(y)$ belong to $L^\infty(\Omega)$ and satisfy

$$0 < \alpha \le a(x), b(y) \le \beta < \infty \tag{4}$$

for any $(x, y) \in \Omega$, where α and β are constants. If the coefficient $a(x)$ is rough, then the solution u to (2) will also be rough; to be specific, u will not in general be in $H^2(\Omega)$ and may not be in $H^{1+\delta}(\Omega)$ for any $\delta > 0$.

In [3, 2], Babuška et al. proposed an approach to this kind of problems based on continuous (or non-conforming) finite element methods. In [3] theoretical proofs were provided for the one dimensional case and arbitrary order approximation. The two dimensional case was considered in [2]. Only second-order accurate elements were considered (piecewise linear elements if A is constant). One of the difficulties in using higher order elements for the continuous Galerkin method is to make the multi-scale spaces conforming. Compared to continuous finite element methods, discontinuous Galerkin (DG) methods do not enforce continuity at the element interfaces which provides an easy way to construct multiscale basis in higher dimensions with high-order elements.

In [18], Yuan and Shu applied the approach of Babuška et al. to the Babuška-Zlámal DG method [4]. They developed a multiscale Babuška-Zlámal DG method based on a non-polynomial basis for Eq. (2) (see [17]). Both theoretical proofs and numerical tests were presented for the one dimensional case. Followed by Yuan and Shu's work, in [16], Wang improved the one dimensional proof of the

multiscale Babuška-Zlámal DG method only assuming that the solution is in $H^1(\Omega)$. In contrast, more regularity was assumed in [18] while proving estimates for the multiscale Babuška-Zlámal DG method.

In this paper we develop a multiscale symmetric interior penalty DG (IP-DG ([10, 19, 1])) method in one and two dimensions. In particular, we prove optimal error estimates in the one dimensional case for arbitrary order approximations. We only assume that the solution is in $H^1(\Omega)$. In the two dimensional case we prove optimal error estimates for the lowest-order (second-order accurate method) multiscale IP-DG method. Moreover, we provide numerical results for higher order elements. Finally, we argue that the recently introduced hybridizable DG methods [8, 7] using piecewise polynomial approximations are convergent for multiscale problems considered here. However, the approximations are at most first-order accurate.

2 Multiscale DG methods in one dimension

First we consider the one dimensional multiscale problem (2) on the domain $[0, 1]$ with boundary condition $u(0) = u(1) = 0$. Let $I_j = (x_{j-\frac{1}{2}}, x_{j+\frac{1}{2}})$, $j = 1, \ldots, N$, be a partition of $[0, 1]$. For simplicity, we assume that the family of partitions are quasi-uniform.

The primal formulation of the IP-DG method [10, 19, 1] is to find $u_h \in V_h$ such that

$$B_h(u_h, v_h) = \int_\Omega f v_h dx, \quad \forall v_h \in V_h, \tag{5}$$

where

$$B_h(u, v) = \sum_{j=1}^{N} \int_{I_j} a\, u_x v_x dx - \sum_{j=0}^{N} \Big([u]_{j-1/2} \{a\, v_x\}_{j-1/2} + \{a\, u_x\}_{j-1/2} [v]_{j-1/2} + \frac{\eta}{h} [u]_{j-1/2} [v]_{j-1/2} \Big), \tag{6}$$

where η is a sufficiently large positive constant for maintaining stability and rates of convergence, and the average $\{u\}$ and jump $[u]$ are defined as follows:

$$[u]_{j-1/2} = u(x^+_{j-1/2}) - u(x^-_{j-1/2}), \quad \{u\}_{j-1/2} = \frac{1}{2}(u(x^+_{j-1/2}) + u(x^-_{j-1/2})), \tag{7}$$

where $u(x^+_{j-1/2})$ and $u(x^-_{j-1/2})$ are the right and left limit of u at the cell boundary $j - 1/2$, $j = 1, \ldots, N$. At the domain boundaries, we have $u(x^-_{1/2}) = 0$ and $u(x^+_{N+1/2}) = 0$.

V_h is the finite element space containing functions which are discontinuous across cell interfaces. For the traditional DG methods, these functions are piecewise polynomials. For the multiscale IP-DG method, the basis functions are constructed to better approximate the solution. The multiscale basis will involve the small scales and may not be polynomials any more. The multiscale IP-DG method is constructed by using such kind of multiscale basis. We will first define the multiscale space V_h and then prove optimal error estimates for the multiscale IP-DG method.

2.1 Multiscale space

In our multiscale IP-DG method, the spaces are constructed below to approximate the solution to (2) (see [18, 3]):

$$S^k = \{\phi \in H^1(0, 1) : -(a\phi_x)_x|_{I_j} \in P^{k-2}(I_j) \text{ for each } j\}. \tag{8}$$

Here we define $P^{-1}(I_j) = \{0\}$. Hence, the multiscale IP-DG method will solve (5) with $V_h = S^k$.

The multiscale approximation space (8) for our model problem (2) is explicitly given by

$$S^k = \left\{ v : v|_{I_j} \in \text{span}\left\{ 1, \int_{x_j}^{x} \frac{1}{a(\xi)} d\xi, \int_{x_j}^{x} \frac{\xi - x_j}{a(\xi)} d\xi, ..., \int_{x_j}^{x} \frac{(\xi - x_j)^{k-1}}{a(\xi)} d\xi \right\} \right\}. \tag{9}$$

Next, we collect some properties of the spaces S^k (see Lemma 4.1 in [3]).

Lemma 1. Given a function $u \in H^1([0,1])$, there is a unique interpolation $u_I \in S^k$ satisfying

$$\begin{array}{l} u_I(x_{j+\frac{1}{2}}) = u(x_{j+\frac{1}{2}}), \quad j = 0, 1, \ldots, n, \\ \int_{I_j} (u - u_I)(x - x_{j-\frac{1}{2}})^l dx = 0, \quad l = 0, \ldots, k-2, \ , j = 1, \ldots, N. \end{array} \tag{10}$$

The following approximation results hold (see Lemma 4.3 in [3]):

Lemma 2. Let u solve (2) and let u_I be its interpolant defined in (10), then for every $j = 1, \ldots, N$ we have

$$\|u - u_I\|_{L^2(I_j)} \leq C(\alpha, \beta) h^{\ell+1} \|f\|_{H^{\ell-1}(I_j)}, \tag{11}$$

$$\|u - u_I\|_{H^1(I_j)} \leq C(\alpha, \beta) h^{\ell} \|f\|_{H^{\ell-1}(I_j)}, \tag{12}$$

where $C(\alpha, \beta)$ is independent of u and h but depends on α, β. Here $1 \leq \ell \leq k$.

Remark 1. There are other ways to prove the above estimates in which one does not need to impose the continuity on the cell boundary and are able to get the same optimal approximation results as in Lemma 2, see [18].

2.2 Error estimates

In this section we prove optimal error estimates for the multiscale IP-DG method. For simplicity, we will consider *quasi-uniform* meshes throughout this paper. We first need to define the energy norm

$$|||v|||^2 := \sum_{j=1}^{N} \|\sqrt{a} v_x\|^2_{L^2(I_j)} + h \sum_{j=0}^{N} \{a v_x\}^2_{j+1/2} + \frac{1}{h} [v]^2_{j+1/2}.$$

We will need the following approximation result using the energy norm.

Lemma 3. Let u solve (2) and let u_I be its interpolant defined in (10), then we have

$$|||u - u_I||| \leq C\, h^{\ell} \|f\|_{H^{\ell-1}([0,1])}.$$

for any $1 \leq \ell \leq k$.

Proof. Since $u - u_I$ vanishes at all the nodes we have

$$|||u - u_I|||^2 = \sum_{j=1}^{N} \|\sqrt{a}(u - u_I)_x\|^2_{L^2(I_j)} + h \sum_{j=0}^{N} (\{a(u - u_I)_x\}^2_{j+1/2}$$

Since a is bounded

$$\begin{aligned}\sum_{j=1}^{N} \|\sqrt{a}(u-u_I)_x\|^2_{L^2(I_j)} \leq & C\,\|(u-u_I)_x\|^2_{L^2([0,1])}\\ \leq & \|u-u_I\|^2_{H^1([0,1])}\\ \leq & C\,h^{2\,\ell}\|f\|^2_{H^{\ell-1}([0,1])}.\end{aligned}$$

In the last inequality we used (12).

To handle the other term. We use the fact that

$$\begin{aligned}&|(au_x)(x^+_{j-1/2}) - (a(u_I)_x)(x^+_{j-1/2})|\\ \leq & |\mathbf{P}^{k-1}(au_x)(x^+_{j-1/2}) - a(u_I)_x(x^+_{j-1/2})| + |\mathbf{P}^{k-1}(au_x)(x^+_{j-1/2}) - au_x(x^+_{j-1/2})|,\end{aligned}$$

where $\mathbf{P}^{k-1}: L^2(I_j) \to P^{k-1}(I_j)$ is the L^2 projection onto $P^{k-1}(I_j)$.

If we use the trace inequality and the approximation properties of $\mathbf{P}^{k-1}$ we have

$$\begin{aligned}&|\mathbf{P}^{k-1}(au_x)(x^+_{j-1/2}) - au_x(x^+_{j-1/2})|\\ \leq & \frac{C}{h^{1/2}}\|\mathbf{P}^{k-1}(au_x) - au_x\|_{L^2(I_j)} + Ch^{1/2}\|(\mathbf{P}^{k-1}(au_x) - au_x)_x\|_{L^2(I_j)}\\ \leq & C\,h^{\ell-1/2}\|D^\ell(au_x)\|_{L^2(I_j)}\\ = & C\,h^{\ell-1/2}\|D^{\ell-1}f\|_{L^2(I_j)}\\ \leq & C\,h^{\ell-1/2}\|f\|_{H^{\ell-1}(I_j)}.\end{aligned}$$

Here we used that the first equation of (2). Therefore, we have

$$h^{1/2}|(\mathbf{P}^{k-1}(au_x)(x^+_{j-1/2}) - au_x(x^+_{j-1/2})| \leq C\,h^\ell\|f\|_{H^{\ell-1}(I_j)},$$

for any $1 \leq \ell \leq k$. Since $u_I \in S^k$ we easily see that $a(u_I)_x|_{I_j} \in P^{k-1}(I_j)$, so by using an inverse estimate we have

$$\begin{aligned}&|\mathbf{P}^{k-1}(au_x)(x^+_{j-1/2}) - a(u_I)_x(x^+_{j-1/2})|\\ \leq & C\,\frac{1}{h^{1/2}}\|\mathbf{P}^{k-1}(au_x) - a(u_I)_x\|_{L^2(I_j)}\\ \leq & C\,\frac{1}{h^{1/2}}\|(au_x) - a(u_I)_x\|_{L^2(I_j)} + C\,\frac{1}{h^{1/2}}\|\mathbf{P}^{k-1}(au_x) - au_x\|_{L^2(I_j)}\\ \leq & C\,\beta\frac{1}{h^{1/2}}\|u_x - (u_I)_x\|_{L^2(I_j)} + C\,\frac{1}{h^{1/2}}\|\mathbf{P}^{k-1}(au_x) - au_x\|_{L^2(I_j)}\\ \leq & C\,h^{\ell-1/2}\|f\|_{H^{\ell-1}(I_j)}.\end{aligned}$$

In the last inequality we used (11).

Therefore,

$$h^{1/2}\,|(au_x)(x^+_{j-1/2}) - (a(u_I)_x)(x^+_{j-1/2})| \leq C\,h^\ell\|f\|_{H^{\ell-1}(I_j)}.$$

In a similar way we can show that

$$h^{1/2}\,|(au_x)(x^-_{j-1/2}) - (a(u_I)_x)(x^-_{j-1/2})| \leq C\,h^\ell\|f\|_{H^{\ell-1}(I_{j-1})}.$$

Using this result and adding the contribution of every node we get

$$h\sum_{j=0}^{N}\{a(u-u_I)_x\}_{j+1/2}^2 \le C\,h^{2\,\ell}\|f\|_{H^{\ell-1}([0,1])}^2.$$

Hence,

$$|||u-u_I|||^2 \le C\,h^{2\,\ell}\|f\|_{H^{\ell-1}([0,1])}^2.$$

The result now follows after we take the square root on both sides. □

Now we can state our main result of this section.

Theorem 2.1. Let $u_h \in V_h = S^k$ be the multiscale IP-DG solution of (5) then we have

$$|||u-u_h||| \le C\,h^k\|f\|_{H^{k-1}([0,1])} \tag{13a}$$

$$\|u-u_h\|_{L^2([0,1])} \le C\,h^{k+1}\|f\|_{H^{k-1}([0,1])}. \tag{13b}$$

Proof. We first prove (13a). To do this we collect some results about the bilinear form $B_h(\cdot,\cdot)$ defined in (6). The first result follows easily by applying the Cauchy-Schwartz inequality and using the fact that a is bounded.

Lemma 4. (Boundedness) There exists a constant C_b such that

$$B_h(w,v) \le C_b\,|||\,w\,|||\,|||v\,||| \quad \forall w,v \in V_h = S^k,$$

The second result concerns the coercivity of the bilinear form.

Lemma 5. (Stability) There exists some constant C_s such that

$$B_h(v,v) \ge C_s\,|||\,v\,|||^2 \quad \forall v \in V_h = S^k. \tag{14}$$

The proof of this lemma, when V_h is the space of piecewise polynomials, is contained in [1] (in the multi-dimensional case as well). The case when $V_h = S^k$ is similar, with the main difference being that we have to apply an inverse estimate to functions of the form av_x. However, by the definition of S^k we have $av_x|_{I_j} \in P^{k-1}(I_j)$ hence we can apply inverse estimates; see the proof of the two-dimensional case in the next section for a similar idea.

Finally, using integration by parts we can easily prove the following Galerkin orthogonality result.

Lemma 6. (Orthogonality) We have the following orthogonality equality

$$B_h(u-u_h,v) = 0 \quad \forall v \in V_h = S^k.$$

Using Lemmas 5, 6 and 4 we obtain

$$C_s\,|||\,u_I-u_h\,|||^2 \le B_h(u_I-u,u_I-u_h) \le C_b\,|||\,u-u_I\,|||\,|||u_I-u_h\,|||\,.$$

Hence,

$$|||u_I-u_h||| \le \frac{C_b}{C_s}\,|||\,u-u_I\,|||\,.$$

Therefore, the triangle inequality gives

$$|||u-u_h||| \le \left(1+\frac{C_b}{C_s}\right)|||\,u-u_I\,|||\,.$$

The inequality (13a) now follows from Lemma 3.

In order to prove (13b), we define the dual problem.

$$-(a\varphi_x)_x = u - u_h, \quad [0,1], \tag{15}$$

with the boundary conditions

$$\varphi(0) = \varphi(1) = 0. \tag{16}$$

Therefore,

$$\begin{aligned}\|u-u_h\|^2_{L^2([0,1])} =& -\int_0^1 (u-u_h)\,(a\varphi_x)_x\,dx \\ =& B_h(u-u_h,\varphi).\end{aligned}$$

In the last equation we used the consistency and symmetry of the IP-DG bilinear form $B_h(\cdot,\cdot)$.

Using Lemma 6 we get

$$\|u-u_h\|^2_{L^2([0,1])} = B_h(u-u_h, \varphi-\varphi_I),$$

where φ_I is the interpolant of φ defined in (10). By Lemma 4 we get

$$\|u-u_h\|^2_{L^2([0,1])} \le C_b \,|||\, u-u_h \,|||\, |||\varphi-\varphi_I \,|||\,.$$

By using Lemma 3 (with $\ell = 1$) we have $|||\varphi-\varphi_I||| \le Ch\|u-u_h\|_{L^2([0,1])}$. We arrive at

$$\|u-u_h\|_{L^2([0,1])} \le C\,h \,|||\, u-u_h \,|||\,.$$

The inequality (13b) now follows from (13a). □

3 Multiscale DG methods in two dimensions

We now consider the two dimensional elliptic multiscale problem (3) on a square domain $[-1,1]^2$. Let $\mathcal{T}_h$ be a collection of *quasi-uniform rectangular* partitions of Ω and $\mathcal{E}_h$ be the collection of edges of the $\mathcal{T}_h$. Define the following inner products

$$\begin{aligned}(v,w)_{\mathcal{T}_h} &= \sum_{K\in\mathcal{T}_h}\int_K v(x,y)\cdot w(x,y)dx\,dy,\\ \langle v,w\rangle_{\mathcal{E}_h} &= \sum_{e\in\mathcal{E}_h}\int_e v(s)\cdot w(s)\,ds.\end{aligned}$$

The IP method finds $u_h \in V_h$ such that

$$B_h(u_h,v_h) = (f,v_h)_{\mathcal{T}_h} \quad \forall v\in V_h, \tag{17}$$

where the bilinear form is defined by

$$B_h(u,v) := (A\nabla u,\nabla v)_{\mathcal{T}_h} - \langle\{\!\{A\nabla u\}\!\},[\![v]\!]\rangle_{\mathcal{E}_h} - \langle\{\!\{A\nabla v\}\!\},[\![u]\!]\rangle_{\mathcal{E}_h} + \frac{\eta}{h}\langle[\![u]\!],[\![v]\!]\rangle_{\mathcal{E}_h}$$

and η is a sufficiently large positive constant. For a scalar valued function u, we define the average $\{\!\{u\}\!\}$ and the jump $[\![u]\!]$ as follows. Let e be an interior edge shared by elements K_1 and K_2. Define the unit normal vectors $\boldsymbol{n}_1$ and $\boldsymbol{n}_2$ on e pointing exterior to K_1 and K_2, respectively. With $u_i := u|_{\partial K_i}$, we set

$$\{\!\{u\}\!\} = \frac{1}{2}(u_1 + u_2), \quad [\![u]\!] = u_1\boldsymbol{n}_1 + u_2\boldsymbol{n}_2 \quad \text{on } e \in \mathcal{E}_h^o, \tag{18}$$

where $\mathcal{E}_h^o$ is the set of interior edges e. For a vector-valued function $\boldsymbol{q}$ we define $\boldsymbol{q}_1$ and $\boldsymbol{q}_2$ analogously and set

$$\{\!\{\boldsymbol{q}\}\!\} = \frac{1}{2}(\boldsymbol{q}_1 + \boldsymbol{q}_2), \quad [\![\boldsymbol{q}]\!] = \boldsymbol{q}_1 \cdot \boldsymbol{n}_1 + \boldsymbol{q}_2 \cdot \boldsymbol{n}_2 \quad \text{on } e \in \mathcal{E}_h^o. \tag{19}$$

For $e \in \mathcal{E}_h^\partial$, the set of boundary edges, we set

$$[\![u]\!] = u\boldsymbol{n}, \quad \{\!\{\boldsymbol{q}\}\!\} = \boldsymbol{q} \quad \text{on } e \in \mathcal{E}_h^\partial, \tag{20}$$

where $\boldsymbol{n}$ is the outward unit normal. We do not require either of the quantities $\{\!\{u\}\!\}$ or $[\![\boldsymbol{q}]\!]$ on boundary edges, and we leave them undefined.

In this section, the high order multiscale IP-DG method for the two dimensional case will be constructed, however the optimal error estimate will be shown only for the second order method.

3.1 Multiscale spaces

The one dimensional approach can be easily expanded to the two dimensional case, i.e. we construct the two dimensional multiscale approximation space as follows (see [18]):

$$S_2^k = \{\phi \in H^1(\Omega) : -(a(x)\phi_x)_x - (b(y)\phi_y)_y|_K \in P^{k-2}(K), \text{ for all } K \in \mathcal{T}_h\}, \tag{21}$$

where (x_K, y_K) is the barycenter of the element K. In particular,

$$S_2^1 = \left\{ v : v|_K \in \text{span}\left\{1, \int_{x_K}^x \frac{1}{a(\xi)}d\xi, \int_{y_K}^y \frac{1}{b(\eta)}d\eta, \right\}\right\},$$

$$\begin{aligned} S_2^2 = \Bigg\{ v : v|_K \in \text{span}\Bigg\{ & 1, \int_{x_K}^x \frac{1}{a(\xi)}d\xi, \int_{y_K}^y \frac{1}{b(\eta)}d\eta, \\ & \int_{x_K}^x \frac{\xi - x_K}{a(\xi)}d\xi, \int_{x_K}^x \frac{1}{a(\xi)}d\xi \int_{y_K}^y \frac{1}{b(\eta)}d\eta, \int_{y_K}^y \frac{\eta - y_K}{b(\eta)}d\eta \Bigg\}\Bigg\}, \end{aligned}$$

and

$$\begin{aligned} S_2^3 = \Bigg\{ v : v|_K \in \text{span}\Bigg\{ & 1, \int_{x_K}^x \frac{1}{a(\xi)}d\xi, \int_{y_K}^y \frac{1}{b(\eta)}d\eta, \\ & \int_{x_K}^x \frac{\xi - x_K}{a(\xi)}d\xi, \int_{x_K}^x \frac{1}{a(\xi)}d\xi \int_{y_K}^y \frac{1}{b(\eta)}d\eta, \int_{y_K}^y \frac{\eta - y_K}{b(\eta)}d\eta, \\ & \int_{x_K}^x \frac{(\xi - x_K)^2}{a(\xi)}d\xi, \int_{x_K}^x \frac{\xi - x_K}{a(\xi)}d\xi \int_{y_K}^y \frac{1}{b(\eta)}d\eta, \int_{x_K}^x \frac{1}{a(\xi)}d\xi \int_{y_K}^y \frac{\eta - y_K}{b(\eta)}d\eta, \int_{y_K}^y \frac{(\eta - y_K)^2}{b(\eta)}d\eta \Bigg\}\Bigg\}. \end{aligned}$$

For $k \geq 4$ it is more difficult to find an explicit formula for the multiscale basis (21).

Hence, the multiscale IP-DG method solves (17) with $V_h = S_2^k$.

3.2 Error estimates

Here we give an error analysis of the lowest-order ($k = 1$) IP-DG method. In order to do so, we define the following energy norm.

$$|||v|||^2 := (A\nabla v, \nabla v)_{\mathcal{T}_h} + \frac{1}{h}\langle [\![v]\!], [\![v]\!]\rangle_{\mathcal{E}_h} + h\langle \{\!\{A\nabla v\}\!\}, \{\!\{A\nabla v\}\!\}\rangle_{\mathcal{E}_h}.$$

We now state our main result.

Theorem 3.1. Let u be the solution of (3) and let $u_h \in V_h = S_2^1$ be the IP-DG approximation, then

$$|||u - u_h||| \leq C\, h \|f\|_{L^2(\Omega)}, \tag{22a}$$

$$\|u - u_h\|_{L^2(\Omega)} \leq C\, h^2 \|f\|_{L^2(\Omega)}. \tag{22b}$$

Before we prove this theorem we will state and prove some important lemmas.

Lemma 7. The following stability result holds

$$|||v|||^2 \leq C B_h(v, v) \quad \forall v \in V_h = S_2^1.$$

Proof. Let $v \in V_h$ then by the definition of $B_h(\cdot, \cdot)$ we get

$$B_h(v, v) = (A\nabla v, \nabla v)_{\mathcal{T}_h} - 2\langle \{\!\{A\nabla v\}\!\}, [\![v]\!]\rangle_{\mathcal{E}_h} + \frac{\eta}{h}\langle [\![v]\!], [\![v]\!]\rangle_{\mathcal{E}_h}. \tag{23}$$

By the arithmetic-geometric mean inequality we get that

$$2\langle \{\!\{A\nabla v\}\!\}, [\![v]\!]\rangle_{\mathcal{E}_h} \leq \frac{1}{\delta h}\langle [\![v]\!], [\![v]\!]\rangle_{\mathcal{E}_h} + h\delta\langle \{\!\{A\nabla v\}\!\}, \{\!\{A\nabla v\}\!\}\rangle_{\mathcal{E}_h}, \tag{24}$$

for any $\delta > 0$. Next, we bound $h\delta\langle \{\!\{A\nabla v\}\!\}, \{\!\{A\nabla v\}\!\}\rangle_{\mathcal{E}_h}$. One can easily show that

$$\langle \{\!\{A\nabla v\}\!\}, \{\!\{A\nabla v\}\!\}\rangle_{\mathcal{E}_h} \leq 2\sum_{K\in\mathcal{T}_h}\int_{\partial K}(A\nabla v)\cdot(A\nabla v). \tag{25}$$

By the definition of V_h, $A\nabla v \in P^1(K)$ on each triangle $K \in \mathcal{T}_h$. Hence, by a standard inverse inequality for the space $P^1(K)$

$$\int_{\partial K}(A\nabla v)\cdot(A\nabla v) \leq C_{\text{inv}}\, h^{-1}\int_K (A\nabla v)\cdot(A\nabla v) \leq C_{\text{inv}}\beta\, h^{-1}\int_K (A\nabla v)\cdot\nabla v.$$

Hence,

$$h\delta\langle \{\!\{A\nabla v\}\!\}, \{\!\{A\nabla v\}\!\}\rangle_{\mathcal{E}_h} \leq 2\delta C_{\text{inv}}\beta(A\nabla v, \nabla v)_{\mathcal{T}_h}. \tag{26}$$

If we plug this result into (24) we get

$$2\langle \{\!\{A\nabla v\}\!\}, [\![v]\!]\rangle_{\mathcal{E}_h} \leq \frac{1}{\delta h}\langle [\![v]\!], [\![v]\!]\rangle_{\mathcal{E}_h} + 2\delta C_{\text{inv}}\beta(A\nabla v, \nabla v)_{\mathcal{T}_h}. \tag{27}$$

Using (23) we obtain

$$\begin{aligned} B_h(v, v) \geq & (A\nabla v, \nabla v)_{\mathcal{T}_h} + \frac{\eta}{h}\langle [\![v]\!], [\![v]\!]\rangle_{\mathcal{E}_h} - \frac{1}{\delta h}\langle [\![v]\!], [\![v]\!]\rangle_{\mathcal{E}_h} \\ & - 2\delta C_{\text{inv}}\beta(A\nabla v, \nabla v)_{\mathcal{T}_h} \\ = & (1 - 2\delta C_{\text{inv}}\beta)(A\nabla v, \nabla v)_{\mathcal{T}_h} + (\frac{\eta}{h} - \frac{1}{\delta h})\langle [\![v]\!], [\![v]\!]\rangle_{\mathcal{E}_h}. \end{aligned}$$

If we choose δ so that $(1-2\delta C_{\rm inv}\beta)\le\frac{1}{2}$ and then if we assume that η is sufficiently large so that $\eta\ge\frac{1}{2\delta}$, then we get

$$(A\nabla v,\nabla v)_{\mathcal{T}_h}+\frac{1}{h}\langle[\![v]\!],[\![v]\!]\rangle_{\mathcal{E}_h}\le C\,B(v,v).$$

Finally, the proof is complete if we use (26). □

The next lemma concerns approximation properties of the space S_2^1.

Lemma 8. Let u solve (3). Then, there exists $v\in V_h=S_2^1$ so that

$$|\!|\!|u-v|\!|\!|\le Ch\|f\|_{L^2(\Omega)}.$$

Proof. We start with a natural transformation. Define

$$\hat{x}:=\int_{-1}^{x}\frac{1}{a(s)}\,ds$$
$$\hat{y}:=\int_{-1}^{y}\frac{1}{b(s)}\,ds.$$

We see that the transformation $(x,y)\to(\hat{x},\hat{y})$ maps $\Omega=[-1,1]\times[-1,1]$ to $\hat{\Omega}=[-1,\int_{-1}^{1}\frac{1}{a(s)}ds]\times[-1,\int_{-1}^{1}\frac{1}{b(s)}]$. Also it maps the rectangle $K\in\mathcal{T}_h$ to a rectangle $\hat{K}$.

Accordingly, for any function u defined on Ω we define a function $\hat{u}$ on $\hat{\Omega}$ by

$$\hat{u}(\hat{x},\hat{y}):=u(x,y).$$

Define $\hat{v}$ to be piece-wise linear function defined on $\hat{\Omega}$ such that $\hat{v}|_{\hat{K}}\in P^1(\hat{K})$ satisfies

$$h_{\hat{K}}\|\nabla(\hat{u}-\hat{v})\|_{L^2(\hat{K})}+\|\hat{u}-\hat{v}\|_{L^2(\hat{K})}\le Ch_{\hat{K}}^2|D^2\widehat{u}|_{L^2(\hat{K})},$$

where $h_{\hat{K}}=\mathrm{diam}(\hat{K})$.

Now define $v\in L^2(\Omega)$, such that on each $K\in\mathcal{T}_h$

$$v(x,y):=\hat{v}(\hat{x},\hat{y}).$$

We easily see that $v\in V_h$.

It is clear that

$$\|u-v\|_{L^2(K)}\le\frac{1}{\alpha}\|\hat{u}-\hat{v}\|_{L^2(\hat{K})}\le Ch_{\hat{K}}^2|D^2\widehat{u}|_{L^2(\hat{K})}.$$

Taking the sum over $K\in\mathcal{T}_h$ we get

$$\|u-v\|_{L^2(\Omega)}\le Ch^2|D^2\widehat{u}|_{L^2(\hat{\Omega})},\tag{28}$$

where we used that $h_{\hat{K}}\le Ch_K$.

We also obtain

$$\begin{aligned}\int_K A\nabla(u-v)\cdot\nabla(u-v)dx\,dy\le&\frac{1}{\alpha}\int_K A\nabla(u-v)\cdot A\nabla(u-v)dx\,dy\\=&\frac{1}{\alpha}\int_{\hat{K}}\nabla(\hat{u}-\hat{v})\cdot\nabla(\hat{u}-\hat{v})\hat{a}(\hat{x})\hat{b}(\hat{y})d\hat{x}\,d\hat{y}\\\le&\frac{\beta^2}{\alpha}\int_{\hat{K}}\nabla(\hat{u}-\hat{v})\cdot\nabla(\hat{u}-\hat{v})d\hat{x}\,d\hat{y}\\\le&Ch_{\hat{K}}^2|D^2\widehat{u}|_{L^2(\hat{K})}^2.\end{aligned}$$

Hence, if we sum over K we get that

$$(A\nabla(u-v),\nabla(u-v))_{\mathcal{T}_h} \leq Ch^2|D^2\widehat{u}|^2_{L^2(\hat{\Omega})}. \tag{29}$$

Finally, we set that

$$\begin{aligned}
&\int_K \nabla(A\nabla(u)) : \nabla(A\nabla(u))dx\ dy \\
=&\int_{\hat{K}} (\frac{1}{\hat{a}}\partial^2_{\hat{x}}\hat{u} + (\frac{1}{\hat{a}}+\frac{1}{\hat{b}})\partial_{\hat{x}}\partial_{\hat{y}}\hat{u} + \frac{1}{\hat{b}}\partial^2_{\hat{y}}\hat{u})\hat{a}\,\hat{b}\,d\hat{x}\ d\hat{y} \\
\leq&\frac{\beta^2}{\alpha}|D^2\hat{u}|^2_{L^2(\hat{K})}.
\end{aligned}$$

Hence,

$$\sum_{K\in\mathcal{T}_h} \|\nabla(A\nabla u)\|^2_{L^2(K)} \leq C\ |D^2\hat{u}|^2_{L^2(\hat{\Omega})}. \tag{30}$$

From the definition of $|||\cdot|||$ we see that

$$\begin{aligned}
|||u-v|||^2 =&(A\nabla(u-v),\nabla(u-v))_{\mathcal{T}_h} + \frac{1}{h}\langle[\![(u-v)]\!],[\![(u-v)]\!]\rangle_{\mathcal{E}_h} \\
&+ h\langle\{\!\{A\nabla(u-v)\}\!\},\{\!\{A\nabla(u-v)\}\!\}\rangle_{\mathcal{E}_h}.
\end{aligned}$$

We bound each term individually. The first term was bounded in (29). For the second term we use the a trace inequality to get

$$\begin{aligned}
\frac{1}{h}\langle[\![(u-v)]\!],[\![(u-v)]\!]\rangle_{\mathcal{E}_h} \leq&\frac{C}{h^2}\|u-v\|^2_{L^2(\Omega)} + C\|\nabla(u-v)\|^2_{L^2(\Omega)} \\
\leq&\frac{C}{h^2}\|u-v\|^2_{L^2(\Omega)} + C\frac{1}{\alpha}(A\nabla(u-v),\nabla(u-v))_{\mathcal{T}_h} \\
\leq&Ch^2|D^2\hat{u}|^2_{L^2(\hat{\Omega})}.
\end{aligned}$$

In the last inequality we used (28) and (29).

If we use a trace inequality we get that

$$\begin{aligned}
&h\langle\{\!\{A\nabla(u-v)\}\!\},\{\!\{A\nabla(u-v)\}\!\}\rangle_{\mathcal{E}_h} \\
\leq&C\sum_{K\in\Omega_h}\|A\nabla(u-v)\|^2_{L^2(K)} + C\,h^2\sum_{K\in\mathcal{T}_h}\|\nabla(A\nabla u)\|^2_{L^2(K)} \\
\leq&\frac{C}{\alpha}(A\nabla(u-v),\nabla(u-v))_{\mathcal{T}_h} + Ch^2\sum_{K\in\mathcal{T}_h}\|\nabla(A\nabla u)\|_{L^2(K)} \\
\leq&C\,h^2|D^2\hat{u}|^2_{L^2(\hat{\Omega})},
\end{aligned}$$

where we used (29) and (30). We also used the fact that $\nabla(A\nabla v)|_K = 0$ for $v\in V_h$ and $K\in\mathcal{T}_h$.

Hence,

$$|||u-v|||^2 \leq Ch^2|D^2\hat{u}|^2_{L^2(\hat{\Omega})}.$$

In order to complete the proof we argue that

$$|D^2\hat{u}|_{L^2(\hat{\Omega})} \leq C\|f\|_{L^2(\Omega)}. \tag{31}$$

We easily see that

$$\begin{aligned} -\frac{1}{\hat{a}}\partial_{\hat{x}}^2\hat{u} - \frac{1}{\hat{b}}\partial_{\hat{y}}^2\hat{u} =& \hat{f} \quad \hat{\Omega}, \\ \hat{u} =& 0, \quad \partial\hat{\Omega}. \end{aligned}$$

By Berstein's Theorem [5] we get that

$$|D^2\hat{u}|_{L^2(\hat{\Omega})} \leq C\|\hat{f}\|_{L^2(\hat{\Omega})}.$$

Finally, using the fact that $\|\hat{f}\|_{L^2(\hat{\Omega})} \leq C\|f\|_{L^2(\Omega)}$ gives (31) and this completes the proof. □

Now we prove Theorem 3.1.

Proof. We first prove (22a). To this end, by Lemma 7 we have

$$|||v - u_h|||^2 \leq C\, B_h(v - u_h, v - u_h),$$

for any $v \in V_h$.

By Galerkin orthogonality of the IP-DG method we have

$$|||v - u_h|||^2 \leq C\, B_h(v - u, v - u_h).$$

Clearly, the $B_h(\cdot,\cdot)$ is a bounded bilinear form. That is,

$$B_h(v - u, v - u_h) \leq C\ |||\, v - u\, |||\ |||v - u_h\ |||\,.$$

Therefore,

$$|||v - u_h||| \leq C\ |||\, v - u\, |||\,.$$

The triangle inequality gives

$$|||u - u_h||| \leq C\ |||\, v - u\, |||\,.$$

Since this holds for any $v \in V_h$, Lemma 8 gives (22a).

In order to prove (22b), we will use a duality argument. We define the problem

$$\begin{aligned} -(a(x)\phi_x(x,y))_x - (b(y)\phi_y(x,y))_y =& (u - u_h)(x,y), \quad (x,y) \in \Omega = [-1,1]^2, & \text{(32a)} \\ \phi(x,y) =& 0, \qquad\qquad\quad (x,y) \in \partial\Omega. & \text{(32b)} \end{aligned}$$

By the adjoint consistency of the IP-DG method we have

$$\|u - u_h\|^2_{L^2(\Omega)} = B_h(u - u_h, \phi) = B_h(u - u_h, \phi - v),$$

for any $v \in V_h$. Here we used Galerkin orthogonality. Hence,

$$\|u - u_h\|^2_{L^2(\Omega)} \leq C\ |||\, u - u_h\, |||\ |||\phi - v||| \leq C\, h\ |||\, u - u_h\, |||\ \|u - u_h\|_{L^2(\Omega)},$$

where we used Lemma 8. The inequality (22b) now follows after we apply (22a). □

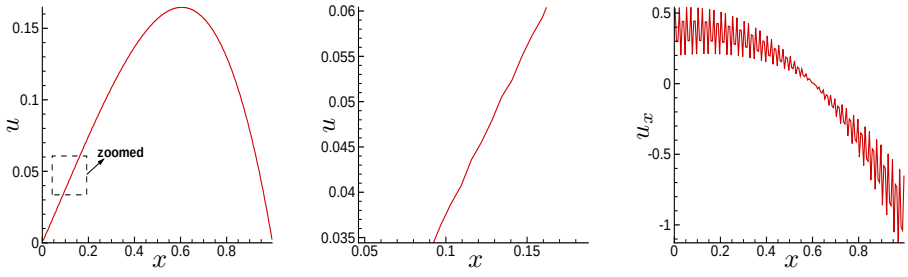

Figure 1: Exact solution of the one dimensional Example 1. Left: u; middle: zoomed part of u; right: u_x.

4 Numerical results

In this section, both one and two dimensional examples are presented to demonstrate that the proposed multiscale IP-DG method can capture the small scales in a very coarse mesh whereas the traditional IP-DG method (i.e. that uses piecewise polynomial spaces) cannot do that.

4.1 One dimensional examples

The first one dimensional example is the same as that in [18]. However the results are computed by the proposed multiscale IP-DG method. The second example is used to show $a(x) = a^\varepsilon(x)$ does not need to have periodicity in $\frac{x}{\varepsilon}$. In both cases, the multi-scale IP-DG method shows the optimal order of convergence for the solution with a very small $\varepsilon = 0.01$ and $\varepsilon = 0.001$ starting from coarse meshes. The stabilization parameter in the IP-DG method is taken as $\eta = 10$.

4.1.1 One dimensional Example 1

Consider the one dimensional multiscale problem Eq. (2) with

$$a(x) = a^\varepsilon(x) = \frac{1}{2 + x + \sin\left(\frac{2\pi x}{\varepsilon}\right)}, \quad f = x, \quad x \in [0, 1]. \tag{33}$$

The exact solution of Eq. (33) with $\varepsilon = 0.01$ is plotted in Fig. 1. The solution itself is oscillatory in the level of ε. However the derivative of the solution is oscillating rapidly (see Fig. 1 right).

We first run this multiscale problem by the traditional IP-DG method with polynomial basis. Table 1 shows the L^2 errors and orders of accuracy for $\varepsilon = 0.01$ and $\varepsilon = 0.001$. We can see that, for $\varepsilon = 0.01$, the traditional IP-DG method starts to converge from the mesh size $N = 320$. However, for $\varepsilon = 0.001$, we cannot see any order of convergence even when the mesh is refined to $N = 640$. This is because the traditional IP-DG method can only have the expected order of convergence when the mesh is refined enough relative to ε, which is consistent with the error estimates for such DG method based on regular piecewise polynomials. We remark that high order IP-DG methods will have the same phenomenon, which we do not show here.

Table 1: L^2 errors and orders of accuracy by the traditional IP-DG method with polynomial basis P^1: One dimensional Example 1.

	$\varepsilon = 0.01$				$\varepsilon = 0.001$			
	$u - u_h$		$q - q_h$		$u - u_h$		$q - q_h$	
N	error	order	error	order	error	order	error	order
10	1.02E-02	–	1.20E-01	–	1.05E-02	–	6.06E-02	–
20	9.82E-03	0.05	1.12E-01	0.10	9.97E-03	0.08	1.56E-01	-1.36
40	9.60E-03	0.03	1.10E-01	0.02	9.89E-03	0.01	1.12E-01	0.48
80	8.85E-03	0.12	1.09E-01	0.01	9.89E-03	0.00	1.12E-01	0.00
160	6.33E-03	0.48	9.67E-02	0.17	8.95E-03	0.14	1.11E-01	0.01
320	2.50E-03	1.34	5.73E-02	0.75	8.99E-03	-0.01	1.11E-01	0.00
640	7.45E-04	1.75	2.98E-02	0.94	8.56E-03	0.07	1.08E-01	0.04

Next we test our multiscale IP-DG method for this multiscale problem with both $\varepsilon = 0.01$ and $\varepsilon = 0.001$. The numerical results are shown in Table 2. We can clearly see the expected order of accuracy which is $(k+1)$th order for u and kth order for q for the multiscale IP-DG method, starting from very coarse meshes.

Table 2: L^2 errors and orders of accuracy by the multiscale IP-DG method: One dimensional Example 1.

	$\varepsilon = 0.01$				$\varepsilon = 0.001$			
S^1	$u - u_h$		$q - q_h$		$u - u_h$		$q - q_h$	
N	error	order	error	order	error	order	error	order
10	1.03E-03	–	4.73E-02	–	1.03E-03	–	4.74E-02	–
20	2.61E-04	1.98	2.36E-02	1.00	2.62E-04	1.97	2.37E-02	1.00
40	6.71E-05	1.96	1.18E-02	1.00	6.62E-05	1.98	1.19E-02	1.00
80	1.68E-05	2.00	5.86E-03	1.01	1.67E-05	1.99	5.93E-03	1.01
160	3.89E-06	2.11	2.80E-03	1.06	4.17E-06	2.00	2.96E-03	1.00
S^2	$u - u_h$		$q - q_h$		$u - u_h$		$q - q_h$	
N	error	order	error	order	error	order	error	order
10	1.16E-05	–	1.01E-03	–	1.15E-05	–	1.01E-03	–
20	1.48E-06	2.97	2.48E-04	2.03	1.46E-06	2.98	2.52E-04	2.00
40	1.89E-07	2.97	6.14E-05	2.01	1.83E-07	2.99	6.28E-05	2.00
80	2.29E-08	3.04	1.51E-05	2.03	2.30E-08	2.99	1.57E-05	2.00
160	2.84E-09	3.01	3.74E-06	2.01	2.94E-09	2.97	3.94E-06	1.99

4.1.2 One dimensional Example 2

In the second example, the coefficient a^ε is not periodic in x or $\frac{x}{\varepsilon}$ and there is no clear scale separation. Consider the multiscale problem with

$$a^\varepsilon(x,\varepsilon) = \frac{1}{2 + x + \sin\left(\frac{\sin x}{\varepsilon}\cos x\right)}, \quad f = -\cos x, \quad x \in [0,1]. \tag{34}$$

We perform the numerical tests by the multiscale IP-DG method on Eq. (34) with $\varepsilon = 0.01$ and $\varepsilon = 0.001$. Table 3 shows the L^2 errors and orders of accuracy. We can again clearly see the expected order of accuracy which is $(k+1)$th order for u and kth order for q, starting from very coarse meshes.

Table 3: L^2 errors and orders of accuracy by the multiscale IP-DG method: One dimensional Example 2.

	$\varepsilon = 0.01$				$\varepsilon = 0.001$			
S^1	$u - u_h$		$q - q_h$		$u - u_h$		$q - q_h$	
N	error	order	error	order	error	order	error	order
10	1.50E-03	–	6.36E-02	–	1.44E-03	–	6.18E-02	–
20	3.51E-04	2.09	2.92E-02	1.12	3.67E-04	1.97	3.09E-02	1.00
40	8.95E-05	1.97	1.50E-02	0.96	9.26E-05	1.99	1.54E-02	1.00
80	2.33E-05	1.94	7.68E-03	0.97	2.33E-05	1.99	7.61E-03	1.02
160	5.93E-06	1.97	3.87E-03	0.99	5.55E-06	2.07	3.59E-03	1.08
S^2	$u - u_h$		$q - q_h$		$u - u_h$		$q - q_h$	
N	error	order	error	order	error	order	error	order
10	8.39E-06	–	5.74E-04	–	7.87E-06	–	5.60E-04	–
20	1.10E-06	2.94	1.38E-04	2.05	9.75E-07	3.01	1.40E-04	2.00
40	1.41E-07	2.97	3.50E-05	1.98	1.27E-07	2.94	3.49E-05	2.00
80	1.77E-08	3.00	8.80E-06	1.99	1.59E-08	2.99	8.51E-06	2.04
160	2.21E-09	3.00	2.20E-06	2.00	1.96E-09	3.02	2.14E-06	1.99

4.2 Two dimensional example

We now consider the two dimensional elliptic multiscale problem Eq. (3) on the domain $[-1,1]^2$ with

$$a(x) = a^\varepsilon(x,\varepsilon) = \frac{1}{4 + x + \sin\left(\frac{x}{\varepsilon}\right)}, \quad b(x) = b^\varepsilon(y,\varepsilon) = \frac{1}{4 + y + \sin\left(\frac{y}{\varepsilon}\right)}, \quad f = x + y. \tag{35}$$

We do not have an explicit representation of the solution, so we computed a reference solution by the spectral Chebyshev collocation method with a mesh 512×512 for $\varepsilon = 0.01$ and $\varepsilon = 0.005$ in order to check the convergence rates of DG methods. Table 4 lists the L^2 errors and orders of convergence of the multiscale IP-DG method. We can see an almost second order convergence for the multiscale IP-DG method with the S_2^1 space and an almost third order convergence with S_2^2, starting from very

coarse meshes. This shows the optimal convergence rates of the multiscale IP-DG method (recall that our proof of optimal convergence is only for S_2^1). Compared to the multiscale IP-DG results, the L^2 errors and orders by the traditional IP-DG method with polynomial spaces P^1 and P^2 are listed in Table 5. For the relative large $\varepsilon = 0.01$, we can see the convergence of the traditional IP-DG method from the mesh size $N = 80$. When ε goes smaller to 0.005, we cannot see a correct order of convergence especially in the P^2 case for the meshes we have tested.

We remark that due to the difficulties of computing a very refined reference solution, we are unable to test a much smaller ε. The smaller the ε is, the bigger advantage of multiscale IP-DG method we should see. This is because the error of the multiscale IP-DG method does not depend on ε, but the traditional IP-DG method can only have convergence when the mesh size is small enough to resolve the ε scale.

Table 4: L^2 errors and orders of accuracy by the multiscale IP-DG method: two dimensional example.

	$\varepsilon = 0.01$		$\varepsilon = 0.005$	
S_2^1				
N	error	order	error	order
10	4.16E-02	–	4.04E-02	–
20	1.28E-02	1.71	1.31E-02	1.63
40	3.56E-03	1.85	3.59E-03	1.87
80	9.42E-04	1.92	9.50E-04	1.92
S_2^2				
10	1.25E-03	–	1.25E-03	–
20	1.82E-04	2.78	1.85E-04	2.75
40	2.54E-05	2.84	2.59E-05	2.84
80	3.57E-06	2.83	3.56E-06	2.86

Table 5: L^2 errors and orders of accuracy by polynomial IP-DG methods: two dimensional example.

	$\varepsilon = 0.01$		$\varepsilon = 0.005$	
P^1				
10	4.98E-02	–	4.97E-02	–
20	2.22E-02	1.16	2.33E-02	1.10
40	1.37E-02	0.69	1.39E-02	0.75
80	5.33E-03	1.36	1.11E-02	0.32
P^2				
10	1.06E-02	–	1.16E-02	–
20	1.09E-02	-0.04	1.06E-02	0.13
40	5.14E-03	1.08	1.08E-02	-0.02
80	7.49E-04	2.78	5.06E-03	1.09

5 DG methods with polynomial basis for multiscale problems

In this section, we are going to show that some DG methods with piecewise constant approximations can approximate the multiscale problem (2) and (3) with first-order accuracy. However, if higher-order accuracy is required then one needs to use multiscale basis in the previous sections.

Falk and Osborn [12] argued that some mixed methods can approximate rough solutions of the problem (3) using piecewise polynomial approximations. Here we argue that the single face-hybridizable (SF-H) method [7] can also approximate rough solutions to (3) using piecewise polynomial approximations. Hybridizable-DG (HDG) methods were recently introduced in [8]. The SF-H [7] method is a special class of HDG methods where on each triangle one only penalizes on exactly one edge. The minimal dissipation local DG (MD-LDG) method [7] is a limiting case of the HDG methods where the penalization parameter is allowed to be infinite (see [8] for more details). We will first give the error estimates for the HDG methods. Then we will show the numerical results by the limiting case MD-LDG method.

5.1 Error estimates for the hybridizable DG methods

In order to define the SF-H method for (3), we need to rewrite (3) in its mixed form. We let

$$A^{-1}\boldsymbol{q} + \nabla u = 0 \tag{36}$$
$$\nabla \cdot \boldsymbol{q} = f \tag{37}$$

where A is given by

$$A(\mathbf{x}) = \begin{pmatrix} a(x) & 0 \\ 0 & b(y) \end{pmatrix}.$$

We let $\{\mathcal{T}_h\}$ be a collection of shape-regular *triangular* partitions of Ω. Let $\mathcal{E}_h$ be the collection of edges of the $\mathcal{T}_h$. We define the function spaces corresponding the lowest-order SF-H method

$$\boldsymbol{\Sigma}_h = \{\boldsymbol{v} \in [L^2(\Omega)]^2 : \ \boldsymbol{v}|_K \in [P^0(K)]^2 \ \forall\, K \in \mathcal{T}_h\}, \tag{38a}$$
$$W_h = \{w \in L^2(\Omega) : \ w|_K \in P^0(K) \ \forall\, K \in \mathcal{T}_h\}, \tag{38b}$$
$$\mathsf{M}_h = \{\mu \in L^2(\mathcal{E}_h) : \ \mu|_e \in P^0(e) \ \forall\, e \in \mathcal{E}_h, \text{ and } \mu = 0 \text{ on } \partial\Omega\}. \tag{38c}$$

The approximation $(\boldsymbol{q}_h, u_h, \lambda_h) \in \boldsymbol{\Sigma}_h \times W_h \times M_h$ is determined by requiring that

$$(A^{-1}\boldsymbol{q}_h, \boldsymbol{v})_{\mathcal{T}_h} - (u_h, \nabla \cdot \boldsymbol{v})_{\mathcal{T}_h} + \langle \lambda_h, \boldsymbol{v} \cdot \boldsymbol{n}\rangle_{\partial\mathcal{T}_h} = 0, \tag{39a}$$
$$-(\boldsymbol{q}_h, \nabla\omega)_{\mathcal{T}_h} + \langle \widehat{\boldsymbol{q}}_h \cdot \boldsymbol{n}, \omega\rangle_{\partial\mathcal{T}_h} = (f, \omega)_{\partial\mathcal{T}_h}, \tag{39b}$$
$$\langle \widehat{\boldsymbol{q}}_h \cdot \boldsymbol{n}, \mu\rangle_{\partial\mathcal{T}_h} = 0, \tag{39c}$$

for all $(\boldsymbol{v}, \omega, \mu) \in \boldsymbol{\Sigma}_h \times W_h \times M_h$, where

$$\widehat{\boldsymbol{q}}_h := \boldsymbol{q}_h + \tau(u_h - \lambda_h)\boldsymbol{n} \quad \text{ on } \partial K \text{ for all } K \in \mathcal{T}_h. \tag{39d}$$

Here $\boldsymbol{n}$ is the outward pointing unit normal to an element $K \in \mathcal{T}_h$. Moreover, we used the following notation

$$\langle \boldsymbol{v} \cdot \boldsymbol{n}, \mu\rangle_{\partial\mathcal{T}_h} := \sum_{K \in \mathcal{T}_h} \int_{\partial K} \boldsymbol{v}(\gamma) \cdot \boldsymbol{n}\, \mu(\gamma)\, d\gamma.$$

The penalty parameters τ is a double-valued constant function on each interior edge of the triangulation $\mathcal{T}_h$. The SF-H method chooses $\tau|_K$ so that it is zero on all but one edge of ∂K. More precisely, it chooses an arbitrary edge e_K^τ of ∂K. Then it sets $\tau = \tau_K > 0$ on e_K^τ but it sets $\tau = 0$ on $\partial K \backslash e_K^\tau$. With such a choice one has the property that $\boldsymbol{q}_h$ and λ_h is independent of τ; see [7]. However, u_h will depend on τ. We note that λ_h is the so-called Lagrange multiplier that approximates u on the edges of the triangulation $\mathcal{T}_h$. In fact, one can locally eliminate $\boldsymbol{q}_h, u_h$ to get a final system for λ_h, then one can recover $\boldsymbol{q}_h, u_h$ element-by-element; see [7, 8].

We now state the main result of this section.

Theorem 5.1. Let u solve (3) and let $(\boldsymbol{q}_h, u_h, \lambda_h) \in \boldsymbol{\Sigma}_h \times W_h \times M_h$ solve (39) then

$$\|\nabla u + A^{-1}\boldsymbol{q}_h\|_{L^2(\Omega)} \leq C\, h \|f\|_{L^2(\Omega)}. \tag{40}$$

Moreover, if $\tau_K \geq \frac{c}{h_K}$ for some constant $c > 0$ and all $K \in \mathcal{T}_h$ then

$$\|u - u_h\|_{L^2(\Omega)} \leq C\, h \|f\|_{L^2(\Omega)}. \tag{41}$$

Proof. By Theorem 2.5 in [7] we have

$$\|A^{-1/2}(\boldsymbol{q} - \boldsymbol{q}_h)\|_{L^2(\Omega)} = C\, h \|\boldsymbol{q}\|_{H^1(\Omega)}.$$

Hence,

$$\begin{aligned}
\|\nabla u + A^{-1}\boldsymbol{q}_h\|_{L^2(\Omega)} \leq & \|A^{-1}(-\boldsymbol{q} + \boldsymbol{q}_h)\|_{L^2(\Omega)} \\
\leq & \frac{1}{\alpha}\|A^{-1/2}(-\boldsymbol{q} + \boldsymbol{q}_h)\|_{L^2(\Omega)} \\
\leq & C\, h \|\boldsymbol{q}\|_{H^1(\Omega)}.
\end{aligned}$$

Using Bernstein's regularity result [5], Falk and Osborn [12] proved that $A\nabla u \in H^1(\Omega)$ although u may not belong to $H^2(\Omega)$. In fact, they proved

$$\|A\nabla u\|_{H^1(\Omega)} \leq C\, \|f\|_{L^2(\Omega)}.$$

Since $\boldsymbol{q} = -A\nabla u$ we have proven (40).

In order to prove (41) we use Corollary 2.7 in [7] that gives

$$\|u - u_h\|_{L^2(\Omega)} \leq C\, h(\|\boldsymbol{q}\|_{H^1(\Omega)} + \|u\|_{H^1(\Omega)}).$$

Here we used our hypothesis $\tau_K \geq \frac{c}{h_K}$ for some constant $c > 0$ and all $K \in \mathcal{T}_h$.

We already argued that $\|\boldsymbol{q}\|_{H^1(\Omega)} \leq \|f\|_{L^2(\Omega)}$. Clearly, by an energy argument we have $\|u\|_{H^1(\Omega)} \leq \|f\|_{L^2(\Omega)}$. This proves (41). □

A few comments are in order. First, it is no surprise that the SF-H method is convergent for (3) since the SF-H method is very similar to standard mixed methods. Also, more general HDG methods (e.g. allowing $\tau = 1$ everywhere) are convergent for (3); however, one needs to trace the effects of the penalty parameters τ on the error $\boldsymbol{q} - \boldsymbol{q}_h$; see [9]. Finally, we point out that higher-order SF-H methods would not give better results since $\boldsymbol{q} \in H^1(\Omega)$ but not in $H^2(\Omega)$.

5.2 Numerical tests by MD-LDG

If we formally set $\tau^- = 0$ and $\tau^+ = \infty$ on all the interior edges of the triangulation $\mathcal{T}_h$, then the HDG method will result in the MD-LDG method (see [8]).

Table 6 shows the numerical results by the piecewise constant MD-LDG method for the one dimensional multiscale problem Example 1 (33). We can see a clear first order convergence for both u and the derivative of u.

We remark that higher order MD-LDG schemes can give the optimal convergence for the derivative of u but not for u. Because the function $a\,u_x$ does not involve the small scale and thus the polynomial basis can well approximate $\boldsymbol{q}$ in the implementation for Eq. (36). In other words, if MD-LDG is implemented in the following way

$$\boldsymbol{q} + \nabla u = 0 \tag{42}$$

$$\nabla \cdot A\boldsymbol{q} = f, \tag{43}$$

we will not be able to see convergence before the small scale is resolved. We do not include these numerical results here.

The numerical results for the two dimensional multiscale problem are listed in Table 7 for $\varepsilon = 0.01$ and $\varepsilon = 0.005$. We can see that the piecewise constant MD-LDG method also shows a first order convergence in the two dimensional case.

Table 6: L^2 errors and orders of accuracy by the MD-LDG with polynomial basis P^0: one dimensional Example 1.

	$\varepsilon = 0.01$				$\varepsilon = 0.001$			
	$u - u_h$		$\boldsymbol{q} - \boldsymbol{q}_h$		$u - u_h$		$\boldsymbol{q} - \boldsymbol{q}_h$	
N	error	order	error	order	error	order	error	order
10	2.21E-02	–	2.69E-02	–	2.23E-02	–	2.69E-02	–
20	1.16E-02	0.93	1.24E-02	1.12	1.18E-02	0.92	1.24E-02	1.12
40	6.01E-03	0.95	5.90E-03	1.07	5.99E-03	0.98	5.88E-03	1.08
80	3.03E-03	0.99	2.86E-03	1.04	3.02E-03	0.99	2.86E-03	1.04
160	1.53E-03	0.98	1.41E-03	1.02	1.51E-03	1.00	1.41E-03	1.03

6 Concluding remarks

In this paper, we developed a multiscale IP-DG method for solving a class of second order elliptic equations with rough coefficients in one- and two-dimensions. Assuming that the solution lies only in H^1, we prove optimal error estimates for arbitrary order approximations for the one dimensional case and optimal error estimates for the second order approximation for the two dimensional case. Numerical tests are performed in both one and two dimensions, demonstrating high order accuracy by the multiscale IP-DG method. In addition, the proof of first order convergence of the HDG method with polynomial basis is given and related numerical test is shown for the MD-LDG method. In future work, we plan to generalize the analysis and develop multiscale DG methods for various elliptic problems.

Table 7: L^2 errors and orders of accuracy by the MD-LDG method with polynomial basis P^0: two dimensional example.

	$\varepsilon = 0.01$		$\varepsilon = 0.005$	
N	error	order	error	order
10	4.14E-01	–	4.16E-01	–
20	2.16E-01	0.94	2.18E-01	0.93
40	1.09E-01	0.99	1.10E-01	0.99
80	5.50E-02	0.99	5.45E-02	1.01
160	2.74E-02	1.01	2.73E-02	1.00

References

[1] D. N. Arnold, *An interior penalty finite element method with discontinuous elements*, SIAM J. Numer. Anal, **39**, 1982, 742–760.

[2] I. Babuška, G. Caloz and J. Osborn, *Special finite element methods for a class of second order elliptic problems with rough coefficients*, SIAM J. Numer. Anal., **31**, 1994, 945–981.

[3] I. Babuška and J. Osborn, *Generalized finite element methods: their performance and their relation to mixed methods*, SIAM J. Numer. Anal., **20**, 1983, 510–536.

[4] I. Babuška and M. Zlámal, *Nonconforming elements in the finite element method with penalty*, SIAM J. Numer. Anal., **10**, 1973, 863–875.

[5] S.N. Bernstein, *Sur la généralisation du probléme de Dirichlet*, Math. Ann., **62**, 1906, 253–271.

[6] Z. Chen and T.Y. Hou, *A mixed multiscale finite element method for elliptic problems with oscillating coefficients*, Math. Comp., **72**, 2002, 541–576.

[7] B. Cockburn, B. Dong and J. Guzmán, *A superconvergent LDG-hybridizable Galerkin method for second-order elliptic problems*, Math. Comp., **77**, 2008, 1887–1916.

[8] B. Cockburn, J. Gopalakrishnan and R. Lazarov, *Unified hybridization of discontinuous Galerkin, mixed, and continuous Galerkin methods for second order elliptic problems*, SIAM J. Numer. Anal., **47**, 2009, 1319–1365.

[9] B. Cockburn, J. Guzmán and H. Wang, *Superconvergent discontinuous Galerkin methods for second-order elliptic problems*, Math. Comp., **78**, 2009, 1–24.

SIAM J. Numer. Anal., **39**, 2001, 264–285.

[10] J. Douglas Jr. and T. Dupont, *Interior Penalty Procedures for Elliptic and Parabolic Galerkin Methods*, Lecture Notes in Phys. 58, Springer-Verlag, Berlin, 1976.

[11] Y.R. Efendiev, T.Y. Hou and X.H. Wu, *The convergence of nonconforming multiscale finite element methods*, SIAM J. Numer. Anal., **37**, 2000, 888–910.

[12] R.S. Falk and J.E. Osborn, *Remarks on mixed finite element methods for problems with rough coefficient*, Math. Comp., **62**, 1994, 1–19.

[13] T.Y. Hou and X.H. Wu, *A multiscale finite element method for elliptic problems in composite materials and porous media*, J. Comput. Phys., **134**, 1997, 169–189.

[14] T.Y. Hou, X.H. Wu and Z. Cai, *Convergence of a multiscale finite element method for elliptic problems with rapidly oscillating coefficients*, Math. Comp., **68**, 1999, 913–943.

[15] P. Langlo and M.S. Espedal, *Macrodispersion for two-phase, immiscible flow in porous media*, Adv. in Water Resources, **17**, 1994, 297–316.

[16] W. Wang, *Multiscale discontinuous Galerkin methods and applications*, Ph.D. Thesis, Brown University, 2008.

[17] L. Yuan and C.-W. Shu, *Discontinuous Galerkin method based on non-polynomial approximation spaces*, J. Comput. Phys., **218**, 2006, 295–323.

[18] L. Yuan and C.-W. Shu, *Discontinuous Galerkin method for a class of elliptic multi-scale problems*, Int. J. Numer. Meth. Fluids, **56**, 2008, 1017–1032.

[19] M.F. Wheeler, *An elliptic collocation-finite element method with interior penalties*, SIAM J. Numer. Anal., **15**, 1978, 152–161.